Restricted Discrete Invariance and Self-Synchronization For Stable Walking of Bipedal Robots

Hamed Razavi[1], Anthony M. Bloch[2], Christine Chevallereau[3] and J. W. Grizzle[4]

Abstract— Models of bipedal locomotion are hybrid, with a continuous component often generated by a Lagrangian plus actuators, and a discrete component where leg transfer takes place. The discrete component typically consists of a locally embedded co-dimension one submanifold in the continuous state space of the robot, called the switching surface, and a reset map that provides a new initial condition when a solution of the continuous component intersects the switching surface. The aim of this paper is to identify a low-dimensional submanifold of the switching surface, which, when it can be rendered invariant by the closed-loop dynamics, leads to asymptotically stable periodic gaits. The paper begins this process by studying the well-known 3D Linear Inverted Pendulum (LIP) model, where analytical results are much easier to obtain. A key contribution here is the notion of *self-synchronization*, which refers to the periods of the pendular motions in the sagittal and frontal planes tending to a common period. The notion of invariance resulting from the study of the 3D LIP model is then extended to a 9-DOF 3D biped. A numerical study is performed to illustrate that asymptotically stable walking may be obtained.

I. INTRODUCTION

While steady progress is being made on the design and analysis of control algorithms for achieving asymptotically stable walking in high-dimensional 3D bipedal robots, the problem remains a very active research area. The control method most widely used on humanoid robots is based on the Zero Moment Point (ZMP) criterion [13], [19], [12], [5], [6], which imposes restrictions on the gaits, such as walking flat-footed. A foot positioning method based on "capture points" has been introduced in Pratt et. al [16], and allows some gaits with partial foot contact with the ground. Both of these methods are based on the Linear Inverted Pendulum model (LIP) [14]. Ames [2] and Greg et. al [7] developed Routhian reduction for fully-actuated 3D bipeds to allow some controllers developed for planar robots an immediate extension to the 3D setting. Grizzle et. al [20], [17], use virtual constraints on an underactuated robot to create an invariant submanifold in the closed-loop hybrid model, and reduce the design of asymptotically stable motions to the study of a low-dimensional system, the hybrid zero dynamics; initial 3D experiments are reported in [4]. These last two methods do not rely on simplified models.

[1]Hamed Razavi and [2]Anthony Bloch are with the Mathematics Department of the University of Michigan, Ann Arbor, MI, USA, {razavi, abloch}@umich.edu

[3] Christine Chevallereau is with LUNAM Université, IRCCyN, CNRS, France, Christine.Chevallereau@irccyn.ec-nantes.fr

[4] J. W. Grizzle is with the Electrical Engineering and Computer Science Department of the University of Michigan, Ann Arbor, MI, USA, grizzle@umich.edu

The aim of the present paper is to identify a low-dimensional submanifold of the switching surface–instead of the entire hybrid model–which, when it can be rendered invariant by the closed-loop dynamics, leads to asymptotically stable periodic gaits. The paper begins this process by studying the well-known 3D LIP model, where analytical results are much easier to obtain. A key contribution here is the notion of *self-synchronization*, which refers to the periods of the pendular motions in the sagittal and frontal planes tending to a common period. The notion of invariance resulting from the study of the 3D LIP model is then extended to a 9-DOF 3D biped, corresponding to a simplified version of the ATRIAS robot designed by Hurst [8], [17], [10]. A numerical study is performed to illustrate that asymptotically stable walking may be obtained.

The paper is organized as follows. In Section II we introduce a discrete invariant gait for the 3D LIP. Then the concept of synchronization is introduced and it is proven that under the discrete invariant gait the 3D LIP will have a periodic motion in which the oscillations in the sagittal and frontal planes are self-synchronized. In Section III, after introducing the model of the 9-DOF 3D biped, inspired by the 3D LIP, we define a discrete invariant gait for the 9-DOF 3D biped. Then we perform a reduction based on this gait, and corresponding to this reduction we define a restricted Poincaré map. After presenting an example of the controllers which enforce the discrete invariant gait, we show that the eigenvalues of the restricted poincare map lie in the unit circle and the walking motion of the biped is stable. The final section includes the concluding remarks.

II. DISCRETE INVARIANCE AND SELF-SYNCHRONIZATION OF THE 3D LIP

In this section we introduce the notion of discrete invariant gait for the 3D LIP and we will show that under this gait the oscillations in the sagittal plane and frontal plane can be self-synchronized. The 3D LIP is known to be a simple walking model that can capture many properties of more complex 3D walking models. For example, in [15] the authors introduce the concept of *capturability* and find what they call *capture regions* based on different types of the 3D LIP model. Later they apply these results to a 12-DOF 3D biped [16]. To generate walking patterns for a humanoid robot, Kajita et. al [14] use the 3D LIP model. Even though the 3D LIP models are simple and have been found to be successful, they have some limitations. For example, the energy loss due to the impact is not usually considered in these models and some
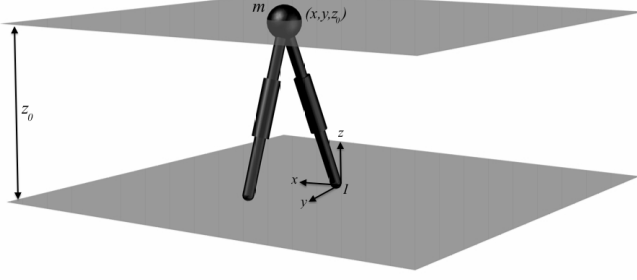
Fig. 1.   3D LIP Biped Model

researchers have modified the LIP model to overcome this limitation [9]. We first define a hybrid model of a 3D LIP biped with massless legs as shown in Figure 1. Let (x, y, z) denote the position of the point mass, m, of the 3D LIP in the inertial coordinate frame, I, centered at the point of support. Assuming that the mass moves in the plane $z = z_0$, $(x, y, \dot{x}, \dot{y})$ defines a set of generalized coordinates for the 3D LIP. Without loss of generality we can assume $m = 1$. The equations of motion in the continuous phase are [14]:

$$\ddot{x} = \omega^2 x$$
$$\ddot{y} = \omega^2 y,$$

where $\omega = \sqrt{g/z_0}$. Also, we define the discrete map as follows

$$
\begin{array}{rcl}
\dot{x}^+ & = & \dot{x}^- \\
\dot{y}^+ & = & -\dot{y}^- \\
x^+ & = & x_{FH}^- \\
y^+ & = & -y_{FH}^-
\end{array}
\quad (x^-, y^-, \dot{x}^-, \dot{y}^-) \in \mathcal{S}, \quad (1)
$$

where (x_{FH}^-, y_{FH}^-) is the position vector from the swing leg end to the point mass represented in I right before the impact and $\mathcal{S}$ is the switching manifold which is defined as

$$\mathcal{S} = \{(x, y, \dot{x}, \dot{y}) | f(x, y) = 0\},$$

for a smooth function $f : \mathcal{S} \to \mathbb{R}$ with rank 1.

The reason that in equation (1) sign of $\dot{y}$ changes after the impact and $y^+ = -y_{FH}^-$ (and not y_{FH}^-) is that by changing the support point we switch the direction of the y coordinate of the inertial frame which is centered at the new support point.

Definition 1. (3D LIP Discrete Invariant Gait) Consider a 3D LIP as described in Figure 1. Suppose that at the beginning of the step $(x, y) = (-x_0, y_0)$ for $x_0 > 0$ and $y_0 > 0$. We say that the 3D LIP takes an (x_0, y_0)−invariant step if the switching manifold is defined as

$$\mathcal{S} = \{(x, y, \dot{x}, \dot{y}) | x^2 + y^2 = x_0^2 + y_0^2\}, \quad (2)$$

and at the moment of double support $(x_{FH}, y_{FH}) = (-x_0, -y_0)$.

Remark 2. This gait is called (x_0, y_0)-invariant because we are assuming that the swing leg is exactly at the desired

position so that $(x_{FH}^-, y_{FH}^-) = (-x_0, -y_0)$ at impact and hence we are assuming that at the beginning of the current step and the next step $(x, y) = (-x_0, y_0)$. We refer to this as *Discrete Invariance* since it only imposes conditions on the discrete phase of motion.

Definition 3. In the 3D LIP, $E_x = \dot{x}^2 - \omega^2 x^2$ and $E_y = \dot{y}^2 - \omega^2 y^2$ are called the orbital energies in the x and y directions [14].

Proposition 4. *Let K_0 be the kinetic energy of the 3D LIP at the beginning (end) of the step. Suppose that the 3D LIP biped completes an (x_0, y_0)-invariant step and K_1 is the kinetic energy of the 3D LIP at the beginning (end) of the next step. We have $K_1 = K_0$.*

Proof. If E_{x_0} and E_{y_0} are the orbital energies at the beginning of the step,

$$
\begin{aligned}
E_{x_0} + E_{y_0} & = \dot{x}_0^2 + \dot{y}_0^2 - \omega^2(x_0^2 + y_0^2) \\
& = 2K_0 - \omega^2 r_0^2, \quad (3)
\end{aligned}
$$

where K_0 is the kinetic energy at the beginning of the step and $r_0^2 = x_0^2 + y_0^2$. On the other hand, if right before the impact $x = x_1$, $y = y_1$, $E_x = E_{x_1}^-$, and $E_y = E_{y_1}^-$, then

$$E_{x_1}^- + E_{y_1}^- = 2K_1^- - \omega^2 r_1^2,$$

where K_1^- is the kinetic energy right before the impact and $r_1^2 = x_1^2 + y_1^2$. However, because by definition of the switching surface at impact $x_1^2 + y_1^2 = r_0^2$, from the equation above

$$E_{x_1}^- + E_{y_1}^- = 2K_1^- - \omega^2 r_0^2. \quad (4)$$

Since, the orbital energies are conserved quantities during each step, $E_{x_0} = E_{x_1}^-$ and $E_{y_0} = E_{y_1}^-$. Therefore, comparing equations (3) and (4), we have $K_1^- = K_0$. By equation (1) there is no loss in velocities due to impact, therefore, $K_1 = K_0$, i.e. the kinetic energy at the beginning of the next step is equal to the kinetic energy at the beginning of the current step. □

Definition 5. (Synchronization) Suppose that at the beginning of a step $E_x > 0$ and $E_y < 0$. The solution in the step is said to be *synchronized* if $\dot{y} = 0$ when $x = 0$.

One can easily check that if at the beginning of the step $(x, y) = (-x_0, y_0)$ and the solution in the step is synchronized, then at the end of the step $(x, y) = (x_0, y_0)$.

Proposition 6. *If the initial conditions are such that the first step of the 3D LIP under the (x_0, y_0)-invariant step is synchronized then the subsequent step will also be synchronized and the 3D LIP follows a 1-periodic motion.*

Proof. The proof follows from the fact that in a synchronized solution the velocities at the end of the step are equal to the velocities at the beginning of the step except that the velocity in the y direction is reversed. □

Definition 7. Suppose that for the 3D LIP at the beginning of the step $x = -x_0 < 0$, $y = y_0 > 0$ and the initial velocities

are $\dot{x}_0 > 0$ and $\dot{y}_0 < 0$. The *synchronization measure* for this step is defined as $L_0 = \dot{x}_0 \dot{y}_0 + \omega^2 x_0 y_0$.

In the next proposition we see that the solution in the step is synchronized if and only if the synchronization measure is zero. Later, to show that the motion is self-synchronized we show that the synchronization measure approaches zero in the subsequent steps.

Proposition 8. *Suppose that the 3D LIP has an (x_0, y_0)-invariant gait with initial velocities $\dot{x} = \dot{x}_0 > 0$ and $\dot{y} = \dot{y}_0 < 0$. Also, suppose that $E_x > 0$ and $E_y < 0$. Let L_0 denote the synchronization measure of this step. The motion of the 3D LIP is 1-periodic if and only if $L_0 = 0$.*

Proof. With the given initial conditions the solution to the 3D LIP system in the continuous phase is

$$x(t) = -x_0 \cosh(\omega t) + \frac{\dot{x}_0}{\omega} \sinh(\omega t) \qquad (5)$$

$$y(t) = y_0 \cosh(\omega t) + \frac{\dot{y}_0}{\omega} \sinh(\omega t). \qquad (6)$$

We want to find $(\dot{x}_0, \dot{y}_0)$ such that the solution that starts from $(-x_0, y_0)$ is synchronized. Therefore, if we set the second equation above to zero, we find the time, t_y, which it takes for $\dot{y}$ to become zero:

$$\tanh(\omega t_y) = -\frac{\dot{y}_0}{y_0 \omega} \qquad (7)$$

Similarly, from equation (5) the time t_x, at which $x = 0$ is found by the following equation:

$$\tanh(\omega t_x) = \frac{x_0 \omega}{\dot{x}_0} \qquad (8)$$

According to the definition of the synchronization, synchronization occurs if $t_x = t_y$, therefore from equations (7) and (8), the motion of the 3D LIP in this step is synchronized if and only if

$$-\frac{\dot{y}_0}{y_0 \omega} = \frac{x_0 \omega}{\dot{x}_0}$$

Hence, from this equation we have synchronization if and only if $\dot{x}_0 \dot{y}_0 + \omega^2 x_0 y_0 = 0$. This result together with Proposition 6 complete the proof. $\square$

So far, we have shown that if the initial conditions are such that $L_0 = 0$, the solution is synchronized. We are also interested in stability in the synchronization. Interestingly, as we will show in the next proposition, the discrete invariant gait can result in self-synchronization of the 3D LIP, that is, eventually the synchronization measure approaches zero.

Proposition 9. *Suppose that the 3D LIP biped model takes an (x_0, y_0)-invariant step with initial velocities $\dot{x} = \dot{x}_0 > 0$ and $\dot{y} = \dot{y}_0 < 0$. Suppose that K_0 is the initial kinetic energy of the system and $K_0 - \omega^2 x_0 y_0 > 0$. Let L_0 and L_1 denote the synchronization measure in the current step and next step, respectively. We have*

$$\lim_{L_0 \to 0} \frac{L_1}{L_0} = -\lambda.$$

where

$$\lambda = 1 - \frac{2\omega^2(y_0^2 - x_0^2)}{\omega^2(y_0^2 - x_0^2) + 2\sqrt{K_0^2 - \omega^4 x_0^2 y_0^2}}. \qquad (9)$$

If $y_0 > x_0$, we have $|\lambda| < 1$.

Proof. One can easily check that the orbital energies, E_x, E_y, and synchronization measure, $L = \dot{x}\dot{y} - \omega^2 xy$ are conserved quantities in the continuous phase of the motion. Also, at impact $x^2 + y^2 = x_0^2 + y_0^2$. Therefore, if the state right before the impact is $(x_1, y_1, \dot{x}_1^-, \dot{y}_1^-)$,

$$(\dot{x}_1^-)^2 - \omega^2 x_1^2 = \dot{x}_0^2 - \omega^2 x_0^2 \qquad (10)$$

$$(\dot{y}_1^-)^2 - \omega^2 y_1^2 = \dot{y}_0^2 - \omega^2 y_0^2 \qquad (11)$$

$$\dot{x}_1^- \dot{y}_1^- - \omega^2 x_1 y_1 = \dot{x}_0 \dot{y}_0 + \omega^2 x_0 y_0 \qquad (12)$$

$$x_1^2 + y_1^2 = x_0^2 + y_0^2. \qquad (13)$$

By Proposition 8, if $L_0 = 0$ the motion is periodic and it can be checked that on this periodic orbit we have the following equations for the orbital energies E_x^* and E_y^*:

$$E_x^* = K_0 + \sqrt{K_0^2 - \omega^4 x_0^2 y_0^2} - \omega^2 x_0^2 \qquad (14)$$

$$E_y^* = K_0 - \sqrt{K_0^2 - \omega^4 x_0^2 y_0^2} - \omega^2 y_0^2. \qquad (15)$$

If $L_0 = 0$ then $x_1 = x_0$, $y_1 = y_0$, $\dot{x}_1^- = \dot{x}_0$ and $\dot{y}_1^- = -\dot{y}_0$. Now, assuming L_0 is infinitesimally small, we have

$$x_1 = x_0 + \delta x_0, \qquad y_1 = y_0 + \delta y_0$$

$$\dot{x}_1^- = \dot{x}_0 + \delta \dot{x}_0, \quad \dot{y}_1^- = -\dot{y}_0 + \delta \dot{y}_0.$$

If we substitute these equations into equations (10-13), we can show that,

$$\lim_{L_0 \to 0} \frac{\delta x_0}{L_0} = \frac{2y_0}{E_{y*} - E_{x*}}. \qquad (16)$$

By definition, if $\dot{x}_1$ and $\dot{y}_1$ are the velocities at the beginning of the next step, $L_1 = \dot{x}_1 \dot{y}_1 + \omega^2 x_0 y_0$. Also, because $\dot{x}\dot{y} - \omega^2 xy$ is conserved during the step, and $(\dot{x}_1, \dot{y}_1) = (\dot{x}_1^-, -\dot{y}_1^-)$, we have $L_0 = -\dot{x}_1 \dot{y}_1 - \omega^2 x_1 y_1$. From these last two equations for L_0 and L_1, and equation (16) we can show that

$$\lim_{L_0 \to 0} \frac{L_1}{L_0} = -1 - \frac{2\omega^2(y_0^2 - x_0^2)}{E_y^* - E_x^*}. \qquad (17)$$

From equations (14) and (15),

$$E_y^* - E_x^* = -2\sqrt{K_0^2 - \omega^4 x_0^2 y_0^2} - \omega^2(y_0^2 - x_0^2),$$

Therefore, substituting this into equation (17) we get equation (9) for λ. From equation (9), if $y_0 > x_0$ we have $|\lambda| < 1$. $\square$

As we will see in the analysis of the Poincaré map, this proposition proves that if $y_0 > x_0$ and $K_0^2 - \omega^4 x_0^2 y_0^2 > 0$, the motion of the 3D LIP is self-synchronized. Inspired by this proposition we define an alternative generalized coordinate for the 3D LIP which allows us to simplify the analysis of stability.

Definition 10. For the 3D LIP define $\alpha = \tan^{-1}(\frac{x}{y})$, $r = \sqrt{x^2 + y^2}$, $\gamma = \dot{x}\dot{y}$ and $v = \sqrt{\dot{x}^2 + \dot{y}^2}$. Then, if $y \neq 0$, (r, α, γ, v) defines a coordinate system for the 3D LIP.

Under the (x_0, y_0)-invariant gait, at impact $r^2 = x_0^2 + y_0^2$. Therefore (α, γ, v) is a coordinate system for the switching manifold $\mathcal{S}$ defined in (2). In the next proposition we study the Poincaré map of the 3D LIP in the coordinate system (α, γ, v).

Proposition 11. *Let $P : \mathcal{S} \to \mathcal{S}$ be the Poincaré map corresponding to the (x_0, y_0)-invariant gait of the 3D LIP. In the coordinate system (α, γ, v) of $\mathcal{S}$, the Poincaré map P has the fixed point $(\alpha^*, \gamma^*, v^*)$ where $\alpha^* = \tan^{-1}(\frac{x_0}{y_0})$, $\gamma^* = -\omega^2 x_0 y_0$ and $v^* = \sqrt{2K_0}$. The Jacobian of the Poincaré map at this fixed point is*

$$DP = \begin{pmatrix} 0 & \star & 0 \\ 0 & -\lambda & 0 \\ 0 & \star & 1 \end{pmatrix},$$

where λ is defined in equation (9).

Proof. Let $P = (P_\alpha, P_\gamma, P_v)^T$. By Proposition 8 under the (x_0, y_0)-invariant gait $\gamma^* = -\omega^2 x_0 y_0$ and $\alpha^* = \tan^{-1}(x_0/y_0)$. By Proposition 9, since at the beginning of each step $L = \gamma + \omega^2 x_0 y_0$,

$$\lim_{L_0 \to 0} \frac{L_1}{L_0} = \frac{\partial P_\gamma}{\partial \gamma}|_{\gamma = \gamma^*}$$
$$= -\lambda$$

where λ is defined in equation (9). Because the legs are massless the value of α at impact won't effect the dynamics of the 3D LIP biped in the next step, hence, $\frac{\partial P}{\partial \alpha} = (0, 0, 0)^T$. Finally, by Proposition 4, $v^* = \sqrt{2K_0}$, and by Proposition 8 under the (x_0, y_0)-invariant gait $P(\alpha^*, \gamma^*, v) = (\alpha^*, \gamma^*, v)$. This proves that the last column of DP is $(0, 0, 1)^T$. $\square$

Corollary 12. *Consider a 3D LIP biped with $E_{x_0} > 0$ and $E_{y_0} < 0$. Let K_0 be the initial kinetic energy of the 3D LIP. Define the constant energy submanifold $\mathcal{S}_{K_0}$ of the switching manifold $\mathcal{S}$ as follows:*

$$\mathcal{S}_{K_0} = \{(\alpha, \gamma, v) \in \mathcal{S} | v = \sqrt{2K_0}\}.$$

Under the (x_0, y_0)-invariant gait, the restricted Poincaré map $P_{K_0} : \mathcal{S}_{K_0} \to \mathcal{S}_{K_0}$ is well defined and the eigenvalues of P_{K_0} are $\{-\lambda, 0\}$ with λ defined in equation (9).

This Corollary shows that by definition of λ, if $y_0 > x_0$, after a perturbation the level of the kinetic energy of the 3D LIP might change but its motion remains self-synchronized.

III. THE 9-DOF 3D BIPED

In this section we generalize the definition of the discrete invariant gait of the 3D LIP to the notion of restricted discrete invariance for a 9-DOF 3D biped which is a simplified model of ATRIAS [17]. Under the invariance assumption for the 9-DOF 3D biped, we perform a reduction and define a restricted Poincaré map which naturally emerges from the reduction. Finally, we define a set of controllers that can enforce the invariance. At the end, simulation results are provided to illustrate that asymptotically stable walking is achieved.

A. Configuration

In this section we study the configuration of the system and different generalized coordinates that we might use to represent the biped. Figure 2 shows ATRIAS [17] and its simplified model, the 9-DOF 3D biped.
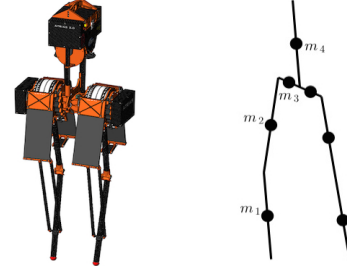

Fig. 2. ATRIAS vs. the 9-DOF 3D Biped

1) Generalized Coordinates: As shown in Figures 3, a set of generalized coordinates that we might use to describe the biped's configuration is $q = (\theta_y, \theta_r, \theta_p, q_1, q_2, q_3, q_4, q_5, q_6)$. The Euler angles $(\theta_y, \theta_r, \theta_p)$, are the yaw, roll and pitch angle of the torso which describe the orientation of torso with respect to the inertial frame. As shown in Figure 3, $(q_1, q_2, q_3, q_4, q_5, q_6)$ are relative angles with respect to the torso and they describe the configuration of the stance and swing legs in a coordinate system attached to the torso. For later reference, we define $\hat{q} = (\theta_r, \theta_p, q_1, q_2, q_3, q_4, q_5, q_6)$.

2) Alternative Coordinates; Quasi-Velocities: Let W denote the inertial (world) frame. Define the coordinate system I to be parallel to W and centered at the support point. Also, let the rotating coordinate system Y be centered at the support point and rotated by θ_y, where θ_y is the yaw angle of the torso with respect to I.

Let r_H and r_F denote the position vector of the hip (see Figure 3) and swing leg end in W, respectively. Define $r_{FH} = r_H - r_F$. Let (x_I, y_I, z_I) and $(x_{FH_I}, y_{FH_I}, z_{FH_I})$ be the coordinates of r_H and r_{FH} in I and let (x, y, z), (x_{FH}, y_{FH}, z_{FH}), (v_x, v_y, v_z) be the coordinates of r_H, r_{FH} and $\dot{r}_H$ in Y.

Lemma 13. *We have $xv_x + yv_y + zv_z = x_I \dot{x}_I + y_I \dot{y}_I + z_I \dot{z}_I$.*

In the next proposition we introduce two alternative sets of generalized coordinates for the 9-DOF 3D biped, which will be used later.

Proposition 14. *If*

$$\xi_1 = (\theta_y, \theta_r, \theta_p, x, y, z, x_{FH}, y_{FH}, z_{FH})$$
$$\zeta_1 = (\dot{\theta}_y, \dot{\theta}_r, \dot{\theta}_p, v_x, v_y, v_z, \dot{x}_{FH}, \dot{y}_{FH}, \dot{z}_{FH}),$$

then (ξ_1, ζ_1) is a coordinate system for $\mathcal{TQ}$, the tangent

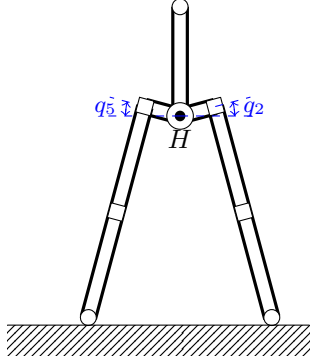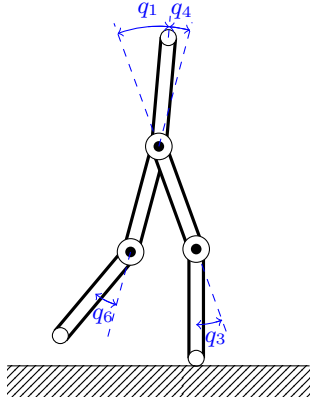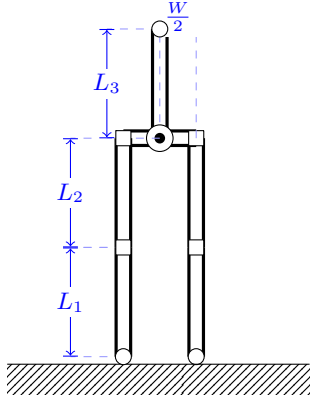Fig. 3. Angle Definitions

Fig. 4. Biped Dimensions

bundle of the configuration space $\mathcal{Q}$. Assuming $y \neq 0$, let

$$\alpha = \tan^{-1}(\tfrac{x}{y}), \quad r = \sqrt{x^2 + y^2}$$
$$\gamma = v_x v_y, \quad v = \sqrt{v_x^2 + v_y^2},$$

with $\alpha \in [-\pi/2, \pi/2]$, and define

$$\xi_2 = (\theta_y, \theta_r, \theta_p, r, \alpha, z, x_{FH}, y_{FH}, z_{FH})$$
$$\zeta_2 = (\dot{\theta}_y, \dot{\theta}_r, \dot{\theta}_p, v, \gamma, v_z, \dot{x}_{FH}, \dot{y}_{FH}, \dot{z}_{FH}).$$

Then (ξ_2, ζ_2) is a coordinate system for $\mathcal{TQ}$. Moreover, if $\hat{\xi}_2 = (\theta_r, \theta_p, r, \alpha, z, x_{FH}, y_{FH}, z_{FH})$, then $(\hat{\xi}_2, \zeta_2)$ is a function of $(\hat{q}, \dot{q})$. Furthermore, if $\mathcal{S} = \{(q, \dot{q}) | z_F(q) = 0\}$,

then,

$$\xi_{\mathcal{S}} = (\theta_y, \theta_r, \theta_p, r, \alpha, z, x_{FH}, y_{FH})$$
$$\zeta_{\mathcal{S}} = (\dot{\theta}_y, \dot{\theta}_r, \dot{\theta}_p, v, \gamma, v_z, \dot{x}_{FH}, \dot{y}_{FH}, \dot{z}_{FH}),$$

defines a coordinate system on $\mathcal{S}$.

Note that ζ_1 and ζ_2 are not the derivatives of ξ_1 and ξ_2. They are called *quasi-velocities* [3].

B. Equations of Motion

Walking is modeled as having continuous and discrete phases. The continuous phase is governed by the Euler-Lagrange equations. The equations of motion in the continuous phase are of the form

$$D(q)\ddot{q} + H(q, \dot{q}) = Bu, \tag{18}$$

where $u_{6 \times 1} = [u_S, u_F]^T$ with u_S and u_F denoting the controllers in the stance and swing legs respectively. Also, $B = [0_{3 \times 6}; I_{6 \times 6}]$. In the discrete phase the velocities are transformed instantly due to the change of support point (from left to right or right to left). Using methodology of [11] which is illustrated for legged robots in [20] we obtain the impulse matrix $\Delta_q(q)$ which maps the velocities $\dot{q}^-$ right before the impact to the velocities immediately after impact, $\dot{q}^+$. In order to use the same set of equations when either the left or the right leg is the stance leg, we implement a matrix R to swap the roles of stance and swing legs. Therefore, setting $x = (q, \dot{q})$, if we rewrite equation (18) and the impulse map in terms of x and $\dot{x}$, we obtain

$$\Sigma = \begin{cases} \dot{x} = f(x) + g(x)u & x^- \notin \mathcal{S} \\ x^+ = \Delta(x^-) & x^- \in \mathcal{S}, \end{cases}$$

where $\Delta(q, \dot{q}^-) = (Rq, R\Delta_q(q)\dot{q}^-)$ and $\mathcal{S}$ is the *switching manifold*, which is defined as

$$\mathcal{S} = \{(q, \dot{q}) | z_F(q) = 0\},$$

where z_F is the height of the swing leg end in W.

Lemma 15. *The kinetic and potential energies of the 9-DOF 3D biped are independent of θ_y [18]. As a result, under the assumption that the controllers are independent of θ_y, if θ_{y_0} is the initial value of θ_y right after the impact, the evolution of $(\hat{q}, \dot{q})$ and $\theta_y - \theta_{y_0}$ are independent of θ_{y_0}.*

Lemma 16. *The impact map is independent of θ_y in the sense that $\dot{q}^+ = \Delta_q(\hat{q})\dot{q}^-$ [18].*

C. Restricted Invariance and Reduction

In this section we introduce a generalization of the discrete invariant gait of the 3D LIP to the 9-DOF 3D biped. This gait enables us to reduce the system dimension to four dimensions and to describe the dynamics in a set of variables which are particularly amenable to analysis.

Definition 17. Let $\mathcal{M}$ be a submanifold of the switching surface $\mathcal{S}$ of the 9-DOF 3D biped. We say that the biped completes an $\mathcal{M}$-invariant step if the solutions starting in $\mathcal{M}$ end in $\mathcal{M}$.

Proposition 18. *Let $\theta_p^d > 0, x_0 > 0, y_0 > 0$ and $q_k^d > 0$, and define the quadruple $\mathcal{P} = (\theta_p^d, x_0, y_0, q_k^d)$. Suppose that the 9-DOF 3D biped completes a step such that at the time of impact,*

(i) $\theta_p = \theta_p^d$, $\theta_r = 0$, $q_3 = q_k^d$, $\dot{\theta}_p = 0$, $\dot{\theta}_r = 0$, $\dot{q}_3 = 0$
(ii) $x_{FH} = -x_0$, $y_{FH} = -y_0$, $q_6 = q_k^d$, $\dot{x}_{FH} = 0$, $\dot{y}_{FH} = 0$, $\dot{q}_6 = 0$.

Then the biped has completed an $\mathcal{M}_\mathcal{P}$-invariant step, where, $\mathcal{M}_\mathcal{P}$ is a submanifold of $\mathcal{S}$ which is the image of the local embedding $f_\mathcal{P} : \mathcal{S} \to \mathcal{S}$ defined as $f_\mathcal{P}(\xi_\mathcal{S}, \zeta_\mathcal{S}) = (\xi_\mathcal{P}, \zeta_\mathcal{P})$, where

$$\xi_\mathcal{P} = (\theta_y, 0, \theta_p^d, r_0, \alpha, z_0, x_0, y_0)$$
$$\zeta_\mathcal{P} = (\dot{\theta}_y, 0, 0, v, \gamma, v_z, 0, 0, 0),$$

for constants r_0 and z_0 which are functions of $\mathcal{P}$. Moreover, $\mathcal{M}_\mathcal{P}$ is 5-dimensional and,

$$\xi_r = (\theta_y, \alpha), \zeta_r = (\gamma, \dot{\theta}_y, v),$$

defines a coordinate system on $\mathcal{M}_\mathcal{P}$. In the closed-loop system the evolution of $(q, \dot{q})$ in the next step is uniquely determined by the value of (ξ_r, ζ_r) at impact.

The goal of the controllers is then that of rendering $\mathcal{M}_\mathcal{P}$ invariant. We will discuss this in more details in Section III-D.

Proof. Step 1. We first show that, by assumptions (i) and (ii) we have $x^2 + y^2 = x_0^2 + y_0^2$ and $z = z_0$, where

$$z_0 = \sqrt{r_1^2 - x_0^2 - y_0^2},$$
$$r_1^2 = L_1^2 + L_2^2 + W^2/4 + 2L_1L_2\cos(q_k^d).$$

From the kinematic equations of the biped,

$$\|\boldsymbol{r}_H\|^2 = L_1^2 + L_2^2 + \frac{W^2}{4} + 2L_1L_2\cos(q_3), \quad (19)$$

$$\|\boldsymbol{r}_{FH}\|^2 = L_1^2 + L_2^2 + \frac{W^2}{4} + 2L_1L_2\cos(q_6). \quad (20)$$

At impact, $x_{FH} = -x_0$, $y_{FH} = -y_0$ and $q_6 = q_k^d$. Therefore, looking at equation (20), we have $x_0^2 + y_0^2 + z_{FH}^2 = r_1^2$. Thus, by definition of z_0, at impact $z_{FH} = z_0$. Consequently, since $z_{FH} = z - z_F$ and at impact $z_F = 0$, we have $z = z_0$. Also, since at impact $q_6 = q_3 = q_k^d$, from equations (19) and (20) at impact $\|\boldsymbol{r}_H\| = \|\boldsymbol{r}_{FH}\|$. Hence, $x^2 + y^2 + z^2 = x_0^2 + y_0^2 + z_0^2$. Since we just showed that at impact $z = z_0$, we have $x^2 + y^2 = x_0^2 + y_0^2$.

Step 2. By Propositions 14 and Step 1, at impact,

$$\xi_2 = (\theta_y, 0, \theta_p^d, r_0, \alpha, z_0, x_0, y_0, z_0)$$
$$\zeta_2 = (\dot{\theta}_y, 0, 0, v, \gamma, v_z, 0, 0, 0),$$

where $r_0 = \sqrt{x_0^2 + y_0^2}$. By equation (19), Lemma 13 and the assumption that at impact $\dot{q}_3 = 0$, we have $v_z = -\frac{1}{z_0}(xv_x + yv_y)$. Therefore, v_z is a smooth function of α, γ and v. So, the reduced coordinates of $\mathcal{M}_\mathcal{P}$ at impact are $\xi_r = (\theta_y, \alpha), \zeta_r = (\gamma, \dot{\theta}_y, v)$. Thus the evolution of $(q, \dot{q})$ in the next step is uniquely determined by the value of (ξ_r, ζ_r) at impact. $\square$

Corollary 19. *If the biped performs an $\mathcal{M}_\mathcal{P}$-invariant step and the controllers are independent of θ_y, then the evolution of $(\alpha, \gamma, \dot{\theta}_y, v)$ and $\theta_y - \theta_{y_0}$ in the next step is uniquely determined by the value of $(\alpha, \gamma, \dot{\theta}_y, v)$ at impact.*

Proof. Since, as stated in Proposition 14, $(\alpha, \gamma, \dot{\theta}_y, v)$ is only a function of $(\hat{q}, \dot{q})$, the proof follows from Lemma 15, Lemma 16 and Proposition 18. $\square$

Corollary 20. *Corresponding to an $\mathcal{M}_\mathcal{P}$-invariant step there exists a 4-dimensional invariant embedded submanifold $\hat{\mathcal{M}}_\mathcal{P}$ of the switching manifold $\mathcal{S}$ such that $(\alpha, \gamma, \dot{\theta}_y, v)$ is a coordinate system of $\hat{\mathcal{M}}_\mathcal{P}$.*

Definition 21. Assuming that $\mathcal{M}_\mathcal{P}$ is invariant, i.e. solutions starting from $\mathcal{M}_\mathcal{P}$ end in $\mathcal{M}_\mathcal{P}$, we can define the $\hat{\mathcal{M}}_\mathcal{P}$-restricted Poincaré map, $\hat{P} : \hat{\mathcal{M}}_\mathcal{P} \to \hat{\mathcal{M}}_\mathcal{P}$, as the function that maps the value of $(\alpha, \gamma, \dot{\theta}_y, v)$ at the end of the current step to its value at the end of the next step.

Remark 22. For simplicity, we assume that the coordinate systems I and Y are right handed when the right leg is the stance leg and they are left handed when the left leg is the stance leg. This choice allows us to analyze the periodic motion and its stability in one step rather than two steps.

Proposition 23. *If the submanifold $\mathcal{M}_\mathcal{P}$ is invariant and the controllers are independent of θ_y, then the restricted Poincaré map has a fixed point $x_r^* = (\alpha^*, \gamma^*, \dot{\theta}_y^*, v^*)$ if and only if the hybrid system has a periodic solution for $(\hat{q}, \dot{q})$ which passes through x_r^*. This periodic orbit is asymptotically stable if and only if x_r^* is an asymptotically stable fixed point of $\hat{P}$. Moreover, if the fixed point x_r^* exists and is asymptotically stable, then θ_y is 2-periodic and is neutrally stable.*

Proof. (*Sketch*) The equivalence of periodicity and asymptotic stability of $(\hat{q}, \dot{q})$ with $\hat{P}$ having an asymptotically stable fixed point follows from Corollary 19. Also, because by Corollary 19, the evolution of θ_y depends on θ_{y_0}, we can show that $\dot{\theta}_y$ is 2-periodic and is neutrally stable (it is not asymptotically stable because θ_{y_0} might change due to a perturbation even though $\theta_y - \theta_{y_0}$ is stable). $\square$

By this proposition, if we find the controllers that render $\mathcal{M}_\mathcal{P}$ invariant, then the periodicity and stability of the motion of the biped can be checked by just looking at the variables $(\alpha, \gamma, \dot{\theta}_y, v)$ at impact. In the next section we discuss such controllers.

D. Controllers

To achieve an $\mathcal{M}_\mathcal{P}$-invariant gait, we find the controllers u_S and u_F such that the conditions in Proposition 18 hold. To this end, we define two goals for our control algorithm: posture control and foot placement. The goal of the posture control is to make y_1 zero and the foot placement algorithm drives y_2 to zero, where

$$y_1 = \begin{pmatrix} \theta_r \\ \theta_p - \theta_p^d \\ q_3 \end{pmatrix}, y_2 = \begin{pmatrix} x_{FH} - x_0 \\ y_{FH} - y_0 \\ q_6 - q_6^d \end{pmatrix}.$$
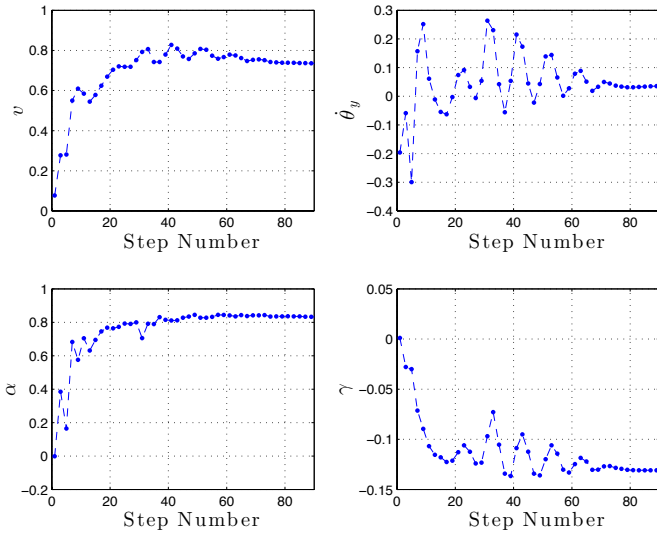
Fig. 5. $(\alpha, \gamma, \dot{\theta}_y, v)$ vs. Step Number. Only the states when the left leg is the stance leg are shown.

To let the swing foot clear the ground, in the first half of the step q_6^d is nonzero and in the second half it is set to zero. For posture control, we only use u_S. If u_F is involved in the posture control then the flight leg would swing in a direction opposite to the torque it applies to the torso. This will disrupt foot placement. Thus, u_F is only used to accomplish the foot placement. As a comparison to the 3D LIP, this foot placement algorithm aims to achieve an (x_0, y_0)-invariant gait. More details of the controllers will appear in a future paper.

E. Simulation Results

Under the above controllers, the biped was able to start walking from zero velocity and exhibit a stable gait. The animations can be found in [1]. Figure 5 shows how the sequence $(\alpha_n, \gamma_n, \dot{\theta}_{y_n}, v_n)$ converges to a fixed point. The dominant eigenvalue of the restricted Poincaré map was found to have an absolute value of 0.96.

IV. CONCLUSION

In this paper, we introduced a discrete invariant gait for the 3D LIP and we proved that under this gait the 3D LIP is self-synchronized and neutrally stable with respect to the kinetic energy. Then we generalized the definition of the discrete invariant gait to the notion of $\mathcal{M}_\mathcal{P}$-invariant gait of a 9-DOF 3D biped. After performing a reduction based on this invariant gait we showed that the periodicity and asymptotic stability of the motion of the 9-DOF 3D biped can be determined by studying a restricted Poincaré map in four variables. Finally, we provided an example of a controller that may satisfy the conditions of the $\mathcal{M}_\mathcal{P}$-invariant gait. By applying this controller to the 9-DOF 3D biped we showed numerically that it performs stable walking. The $\mathcal{M}_\mathcal{P}$-invariant gait introduced here is not limited to the particular 9-DOF 3D biped which was studied here. For example, we tested this gait on a half scale biped model

of the 9-DOF 3D biped we studied here and were able to achieve stable walking.

REFERENCES

[1] 3D Biped Animations. http://www-personal.umich.edu/~razavi/publications.html.
[2] Aaron D. Ames, Robert D. Gregg, and Mark W. Spong. A geometric approach to three-dimensional hipped bipedal robotic walking. In *Decision and Control, 2007 46th IEEE Conference on*, pages 5123–5130. IEEE, 2007.
[3] Anthony M. Bloch, Jerrold E. Marsden, and Dmitry V. Zenkov. Quasivelocities and symmetries in non-holonomic systems. *Dynamical systems*, 24(2):187–222, 2009.
[4] Brian G. Buss, Alireza Ramezani, Kaveh Akbari Hamed, Brent A. Griffin, Kevin S Galloway, and Jessy W Grizzle. Preliminary walking experiments with underactuated 3d bipedal robot marlo.
[5] A. Goswami. Foot rotation indicator (FRI) point: A new gait planning tool to evaluate postural stability of biped robots. In *Int. Conf. on Robotics and Automation*, pages 47–52. IEEE, May 1990.
[6] A. Goswami. Postural stability of biped robots and the foot-rotation indicator (FRI) point. *International Journal of Robotics Research*, 18(6):523–533, June 1999.
[7] Robert D. Gregg and Mark W. Spong. Reduction-based control with application to three-dimensional bipedal walking robots. In *American Control Conference, 2008*, pages 880–887. IEEE, 2008.
[8] J. A. Grimes and J. W. Hurst. The design of ATRIAS 1.0 a unique monopod, hopping robot. pages 548–554, July 2012.
[9] Jessy W. Grizzle, Christine Chevallereau, Ryan W Sinnet, and Aaron D Ames. Models, feedback control, and open problems of 3d bipedal robotic walking. *Automatica*, 2014.
[10] Christian Hubicki, Jesse Grimes, Mikhail Jones, Daniel Renjewski, Alexander Spröwitz, Andy Abate, and Jonathan Hurst. Atrias: Enabling agile biped locomotion with a template-driven approach to robot design. *IJRR*, 2014.
[11] Yildirim Hurmuzlu and Dan B. Marghitu. Rigid body collisions of planar kinematic chains with multiple contact points. *The International Journal of Robotics Research*, 13(1):82–92, 1994.
[12] S. Kajita, F. Kanehiro, K. Kaneko, K. Fujiwara, K. Harada, K. Yokoi, and H. Hirukawa. Biped walking pattern generator allowing auxiliary zmp control. In *Proc. 2006 IEEE/RSJ Int. Conf. on Intelligent Robots and Systems*, pages 2993–2999, 2006.
[13] S. Kajita, M. Morisawa, K. Harada, K. Kaneko, F. Kanehiro, K. Fujiwara, and H. Hirukawa. Biped walking pattern generation by using preview control of zero-moment point. volume 2, pages 1620–1626, September 2003.
[14] Shuuji Kajita, Fumio Kanehiro, Kenji Kaneko, Kazuhito Yokoi, and Hirohisa Hirukawa. The 3d linear inverted pendulum mode: A simple modeling for a biped walking pattern generation. In *Intelligent Robots and Systems, 2001. Proceedings. 2001 IEEE/RSJ International Conference on*, volume 1, pages 239–246. IEEE, 2001.
[15] Twan Koolen, Tomas De Boer, John Rebula, Ambarish Goswami, and Jerry Pratt. Capturability-based analysis and control of legged locomotion, part 1: Theory and application to three simple gait models. *The International Journal of Robotics Research*, 31(9):1094–1113, 2012.
[16] Jerry Pratt, Twan Koolen, Tomas De Boer, John Rebula, Sebastien Cotton, John Carff, Matthew Johnson, and Peter Neuhaus. Capturability-based analysis and control of legged locomotion, part 2: Application to m2v2, a lower-body humanoid. *The International Journal of Robotics Research*, 31(10):1117–1133, 2012.
[17] Alireza Ramezani, Jonathan W. Hurst, Kaveh Akbari Hamed, and J. W. Grizzle. Performance analysis and feedback control of atrias, a three-dimensional bipedal robot. *Journal of Dynamic Systems, Measurement, and Control*, 136(2):021012, 2014.
[18] Mark W. Spong and Francesco Bullo. Controlled symmetries and passive walking. *Automatic Control, IEEE Transactions on*, 50(7):1025–1031, 2005.
[19] M. Vukobratović, B. Borovac, and V. Potkonjak. ZMP: A review of some basic misunderstandings. 3(2):153–175, 2006.
[20] Eric R. Westervelt, Jessy W. Grizzle, Christine Chevallereau, Jun Ho Choi, and Benjamin Morris. *Feedback control of dynamic bipedal robot locomotion*. Citeseer, 2007.